Journal of Solid State Chemistry **168,** 126–133 (2002)
doi:10.1006/jssc.2002.9699

Mössbauer Investigation of ^{57}Fe-Doped Ni(III) Perovskites $ANi_{0.98}Fe_{0.02}O_3$ (A=Pr, Nd, Sm, Y, Lu, Tl) versus Temperature

Seung-Joo Kim,* Igor Presniakov,† Gerard Demazeau,*,[1] Konstantin Pokholok,† Alexey Baranov,† Alexey Sobolev,† Denis Pankratov,† and Nikolay Ovanesyan‡

*Institut de Chimie de la Matiere Condensee de Bordeaux (UPR CNRS 9048), 87 Avenue A. Schweitzer—33608 Pessac Cedex, France; †Department of Chemistry, Lomonosov University, 119899 Moscow, Russia; and ‡Institute of Problems of Chemical Physics, Chernogolovka, Russia

Received January 24, 2002; in revised form May 27, 2002; accepted July 15, 2002

Nickelates $ANiO_3$ (A = Pr, Nd, Sm, Lu, Y, Tl) containing Mössbauer probe ^{57}Fe atoms were synthesized. In the case of nickelates with larger rare earth (A = Pr, Nd, Sm) the Mössbauer spectra confirm that ferric ions are located in single type of crystallographic positions. On the contrary, the spectra of $ANi_{0.98}Fe_{0.02}O_3$ with small cations (A = Lu, Y, Tl) can be described as a superposition of two sub-spectra which indicate that ^{57}Fe probe atoms are simultaneously stabilized in two non-equivalent crystallographic positions. These results have been interpreted in terms of partial charge disproportionation of Ni^{3+} cations associated with the electronic localization in monoclinic distorted Lu, Y, Tl nickelates. The modification of ^{57}Fe spectra for $TlNi_{0.98}Fe_{0.02}O_3$ as a function of temperature has shown that this charge disproportionation occurs in varying degrees, corresponding to the charge states $Fe^{(3+\sigma)+}$ and $Fe^{(3-\sigma')+}$. On the contrary, the spectra for Lu and Y nickelates show that charge variation (σ, σ') for dopant Fe(1) and Fe(2) cations does not depend on temperature.

Key Words: **Mössbauer spectroscopy; perovskite; trivalent nickel; charge disproportionation.**

INTRODUCTION

Nickel(III) perovskites $ANiO_3$ (with A = rare earth) have been earlier prepared at normal pressure conditions for $LaNiO_3$ (1) and under high oxygen pressure for A (= Nd → Lu and Y) (2). Recently—in order to point out the role of the A^{3+}–O bond on the physical properties of the $ANiO_3$ nickelates—the $TlNiO_3$ perovskite has been synthesized and studied (3). The evolution of the Néel temperature T_N is generally correlated for the $ANiO_3$ series (A = rare earth and Y) to the decreasing value of the Ni–O–Ni angle induced by the improvement of the structural distortion of the perovskite lattice. Such a distortion increases from La^{3+} to Lu^{3+} due to the shrinking of the A^{3+} size. The average Ni–O–Ni bond angle for $TlNiO_3$ (147.6°) is comparable to that for $YNiO_3$ (147.3°), but a large difference of the T_N value is observed between these two oxides: T_N ($YNiO_3$) = 145 K, T_N ($TlNiO_3$) = 105 K. Such a difference is explained by the strong covalent Tl–O bond compared to the Y–O ones (3). Along the Tl–O–Ni bonds the electron density is increasingly kept in more covalent Tl–O bonds, thus weakening the magnetic interactions between Ni(III) cations.

During these last 10 years the physical properties of such perovskites have been intensively investigated (4). Due to the adopted low-spin electronic configuration ($t_{2g}^6 e_g^1$), Ni(III), in an oxygen lattice, is basically a two-fold degenerated state as high-spin Fe(IV) ($t_{2g}^3 e_g^1$) or high-spin Mn(III) ($t_{2g}^3 e_g^1$). This electronic configuration with the single e_g electron can lead to different instabilities like the cooperative Jahn–Teller effect as observed for Mn(III) oxides (5) or orbital ordering as suggested for explaining the complex magnetic structure adopted for $NdNiO_3$ and $SmNiO_3$ (6). Due to the respective depth of the 3d levels relative to the O_{2p} one when the oxidation state (n+) is increased the charge transfer fluctuations $O^{2-} \rightarrow M^{n+}$ can occur and the properties of such transition metals oxides can be strongly dominated by oxygen–hole character (7).

Recently, through high-resolution neutron and synchrotron diffraction techniques, the changes of symmetry from orthorhombic in the metallic phase to monoclinic in the insulating phase have been observed in $ANiO_3$ lattices for the small rare-earth A^{3+} (A = Ho, Y, Er, Tm, Yb, Lu). It has been showed that in the insulating regime ($T < T_{IM}$) the above perovskites contain two chemically different Ni(1) and Ni(2) cations. The significantly different mean Ni–O bond distances observed for Ni(1) and Ni(2) cations in the monoclinic phases suggest the presence of a partial charge

[1] To whom correspondence should be addressed. Fax: 33-(0)5-56-84-27-10. E-mail: demazeau@icmcb.u-bordeaux.fr.

0022-4596/02 $35.00

disproportionation: $2Ni^{3+} \leftrightarrow Ni^{(3-\alpha')+}(1) + Ni^{(3+\alpha)+}(2)$ with $\alpha(\alpha')$ increasing toward unity with increasing the size difference between the two kinds of Ni(1)O_6 and Ni(2)O_6 octahedra (8, 9).

The existence of two different Ni(1) and Ni(2) sites in $ANiO_3$ lattices for the small rare earth nickelates has been recently confirmed by a Mössbauer study of ^{57}Fe-doped nickelates $ANi_{0.98}{}^{57}Fe_{0.02}O_3$ (A = Y, Lu, Tl) at 300 K (10). The ^{57}Fe spectra of these nickelates can be described as a superposition of two sub-spectra which indicate that ^{57}Fe probe atoms are stabilized in two non-equivalent crystallographic positions. On the contrary, the spectrum of large rare-earth nickelates, $ANi_{0.98}{}^{57}Fe_{0.02}O_3$ (A = Pr, Nd, Sm), has confirmed the existence of only one nickel chemical species in such lattices and consequently the non-existence of a disproportionation phenomenon with the large rare earths. At $T \ll T_N$ the existence of two different sub-spectra corresponding to two Fe(III) sites, mainly characterized by two different hyperfine fields ($H_1 = 450-430$ kOe and $H_2 = 22-15$ kOe), but with δ and Δ values approximately constant, has underlined that in the ordered magnetic domain, as proposed previously through a neutron diffraction study, an orbital ordering of the e_g^1 orbitals leads to two different sites characterized by a different magnetic surrounding (11).

The objective of this Mössbauer study was, using ^{57}Fe probe, to investigate the $ANi_{0.98}Fe_{0.02}O_3$ perovskites at different temperatures in order to evaluate the evolution of the electronic phenomena taking place in such lattices—in particular the charge disproportionation.

EXPERIMENT

The $ANi_{0.98}{}^{57}Fe_{0.02}O_3$ (A = Y, Lu and Tl) polycrystalline samples were prepared in two steps. The first one involved the preparation of the precursors, mainly $Ni_{0.98}{}^{57}Fe_{0.02}O$. Such a preparation has been described in the paper involving the Mössbauer study of $ANi_{0.98}{}^{57}Fe_{0.02}O_3$ at 300 K (10). The second step was a high oxygen pressure treatment of the precursors A_2O_3 and $Ni_{0.98}{}^{57}Fe_{0.02}O$ with $KClO_3$ used as oxygen source in a belt-type equipment. The optimized experimental conditions, leading to a single perovskite phase and KCl (resulting from the thermal decomposition of $KClO_3$) were 6 GPa, 900°C, 10 min for A^{3+} = Lu, Y. On the contrary, due to the thermal instability of Tl_2O_3 the selected experimental conditions for A^{3+} = Tl were 7.5 GPa, 700°C, 5 min. $ANi_{0.98}{}^{57}Fe_{0.02}O_3$ (A = Pr, Nd and Sm) was prepared by the high oxygen pressure treatment of precursors obtained from sol–gel method. Appropriate amounts of A_2O_3 (A = Pr, Nd, Sm), $Ni(NO_3)_2 \cdot 6H_2O$, ^{57}Fe metal and citric acid were dissolved in dilute nitric acid. The solution was evaporated with keeping its pH 5–6 until a blue gel was obtained. The gel was decomposed at 750°C for 6 h in air. The resulting powders were heated at 850°C for 4 days under an oxygen pressure of 100 MPa.

The ^{57}Fe Mössbauer spectra were recorded at various temperatures using a conventional constant acceleration Mössbauer spectrometer. The radiation source ^{57}Co(Rh) was kept at room temperature. All isomer shifts refer to the α-Fe absorber at 300 K.

RESULTS AND DISCUSSION

^{57}Fe Mössbauer spectra of $ANi_{0.98}{}^{57}Fe_{0.02}O_3$ nickelates with large rare-earth cations (A = Pr, Nd, and Sm) at $T = 300$ K consist of a single unresolved quadrupole doublet (Fig. 1) with isomer shift (δ) value (Table 1) corresponding to Fe(III) cations in high-spin state located in the oxygen octahedral surrounding. The small values of the quadrupole splitting (Δ) may be considered as evidence for the high symmetry of the nearest anionic surrounding

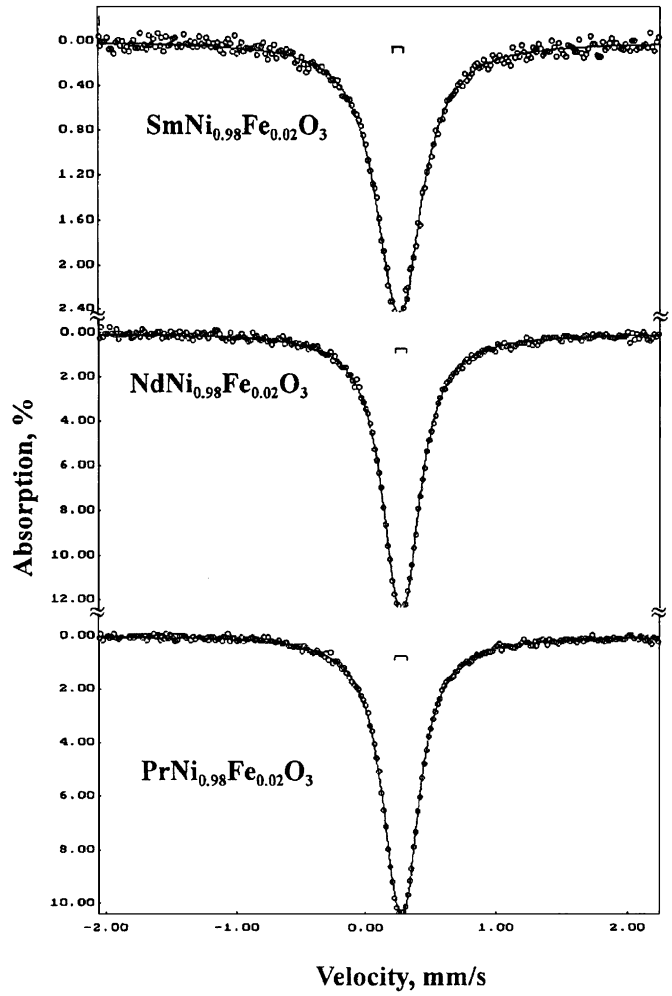

FIG. 1. ^{57}Fe Mössbauer spectra of $ANi_{0.98}{}^{57}Fe_{0.02}O_3$ (A = Nd, Sm, Pr) at 300 K.

TABLE 1
Mössbauer Parameters for $A\mathrm{Ni}_{0.98}{}^{57}\mathrm{Fe}_{0.02}\mathrm{O}_3$ (A = Nd, Pr, Sm) at $T = 300$ K

Compounds	δ (mm/s) (± 0.01)	Δ (mm/s) (± 0.01)	Γ (mm/s) (± 0.01)	$d\delta/dT \times 10^{-4}$ (mm/s K)
$\mathrm{PrNi}_{0.98}\mathrm{Fe}_{0.02}\mathrm{O}_3$	0.23	0.08	0.29	−4.5
$\mathrm{NdNi}_{0.98}\mathrm{Fe}_{0.02}\mathrm{O}_3$	0.22	0.06	0.28	−4.3
$\mathrm{SmNi}_{0.98}\mathrm{Fe}_{0.02}\mathrm{O}_3$	0.26	0.11	0.28	−5.1

of iron atoms. This result is in agreement with the nearly regular NiO_6 octahedra observed in the first members of the $A\mathrm{NiO}_3$ family (9). It should be noted that δ values for the above nickelates are smaller than those in the rare-earth orthoferrites: $PrFeO_3$ (0.35 mm/s), $NdFeO_3$ (0.37 mm/s) and $SmFeO_3$ (0.39 mm/s) (12). This feature can be correlated with the increase of the ionicity of the Fe^{III}–O bonds [$d_{\mathrm{Fe(III)–O}} \approx 2.03$ Å] resulting from the presence of more covalent competing Ni^{III}–O bonds [$d_{\mathrm{Ni(III)–O}} \approx$ 1.94 Å]. Such inductive effect may modify the isomer shift values for ^{57}Fe(III) ions in microdoped $A\mathrm{NiO}_3$ samples as compared to δ values in iron oxides (13).

Figure 2 shows the temperature dependence of the isomer shift for ^{57}Fe probe atoms in Pr, Nd and Sm nickelates. The δ values exhibit the usual increase, with respect to the room-temperature values, due to the second-order Doppler effect (14). The temperature coefficient ($d\delta/dT$), calculated from the slope of the temperature shift for the above nickelates, are given in Table 1. These values are in agreement with the theoretical slope $d\delta/dT = 7.3 \times 10^{-4}$ mm/s K obtained for a solid below its Debye temperature (14). The quadrupole splitting values are essentially the same as those at room temperature (Fig. 3). This behavior is generally observed for high-spin Fe(III) compounds in which only the lattice contribution (eq^{lat}) to the electric field gradient (EFG) affects the quadrupole splitting.

The spectra of $A\mathrm{Ni}_{0.98}{}^{57}\mathrm{Fe}_{0.02}\mathrm{O}_3$ nickelates with small cations (A = Lu, Y and Tl) can be described as a superposition of two quadruple doublets (Fig. 4), which could indicate that dopant Fe ions are located in two non-equivalent crystallographic sites. It should be noted that chemical shifts for both iron states (Table 2) correspond to the formal three-valent ferric cations in the oxide compounds (13). The observed difference between δ_1 and δ_2 values may be explained by the difference in the Fe–O bonds covalency in $Fe(1)O_6$ and $Fe(2)O_6$ polyhedra. These results are consistent with the recently obtained neutron diffraction data for undoped $A\mathrm{NiO}_3$ samples, which indicate that in the nickelates with small rare-earth cations A (= Ho → Lu and Y) the lattice symmetry is lowered to the monoclinic one ($P2_1/n$), and thus suggest the "splitting" of the Ni positions: $Ni^{(3-\alpha')+}$(1) and $Ni^{(3+\alpha)+}$(2) (8, 9). It is reasonable to assumed that the concentration of electrons occupying the antibonding orbitals will be higher in the expanded $F(1)O_6$ octahedra than in the smaller $Fe(2)O_6$

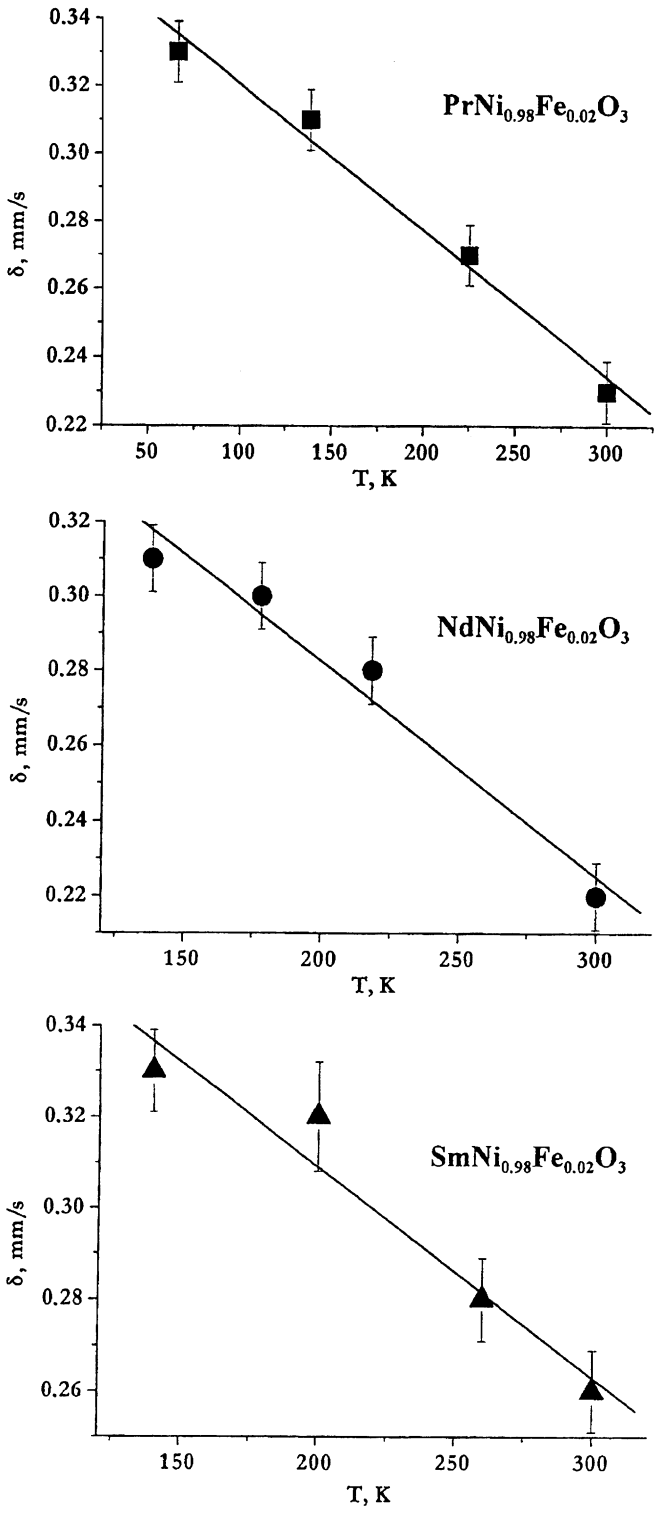

FIG. 2. Temperature dependence of the ^{57}Fe isomer shift (δ) for $A\mathrm{Ni}_{0.98}{}^{57}\mathrm{Fe}_{0.02}\mathrm{O}_3$ (A = Pr, Nd, Sm).

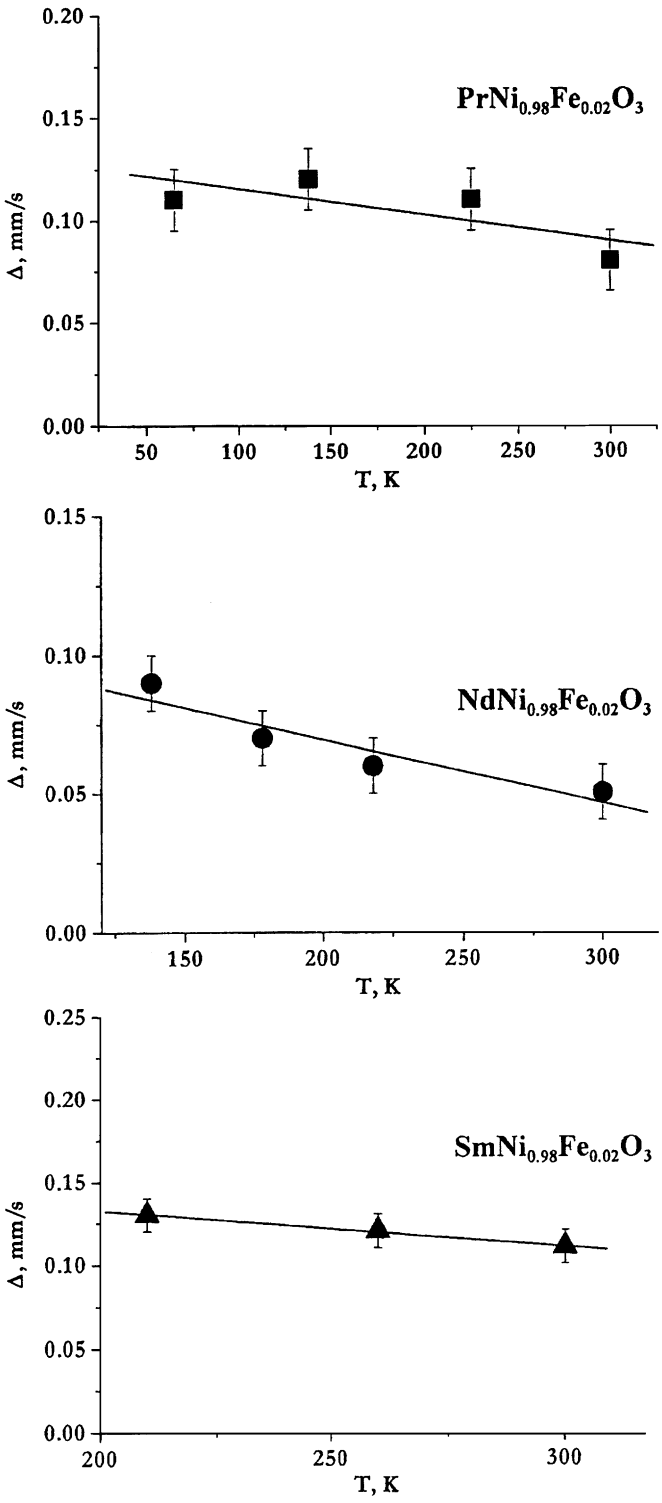

FIG. 3. Temperature dependence of the ^{57}Fe quadrupole splitting (Δ) for $A\mathrm{Ni}_{0.98}{}^{57}\mathrm{Fe}_{0.02}\mathrm{O}_3$ (A = Pr, Nd, Sm).

ones. Given that the decrease of formal oxidation state (n) of Fe^{n+} cations increases their isomer shift (13), the quadrupole doublet with larger δ_1 (Table 2) may be related to $\mathrm{Fe}^{(3-\sigma')+}(1)$ cations which substitute the nickel ones on expanded $\mathrm{Ni}^{(3-\alpha')+}\mathrm{O}_6$ octahedra. In terms of this model, the second quadrupole doublet with a smaller isomer shift (δ_2) corresponds to $\mathrm{Fe}^{(3+\sigma)+}(2)$ cations which substitute the nickel in contracted $\mathrm{Ni}^{(3+\alpha)+}\mathrm{O}_6$ octahedra.

The relative contributions of Fe(1) and Fe(2) sub-spectra (S) are unequal and constant within the experimental error whatever the $A\mathrm{Ni}_{0.98}{}^{57}\mathrm{Fe}_{0.02}\mathrm{O}_3$ lattices (Table 2). Such an unequal distribution of Fe ions may be induced by the steric factors: the trivalent iron cations prefer Ni(1) sites rather than the Ni(2) ones since the average $\mathrm{Fe}^{\mathrm{III}}$–O bonds distance (2.03 Å) in FeO_6 octahedra for ferric oxides is closer to the average bond distance of Ni(1)–O (2.00 Å) than to that of Ni(2)–O bonds (1.92 Å) in the $A\mathrm{NiO}_3$ (9). It seems to be surprising that the relative contributions of Fe(1) and Fe(2) sub-spectra remains almost invariable for nickelates with different extent of monoclinic distortion.

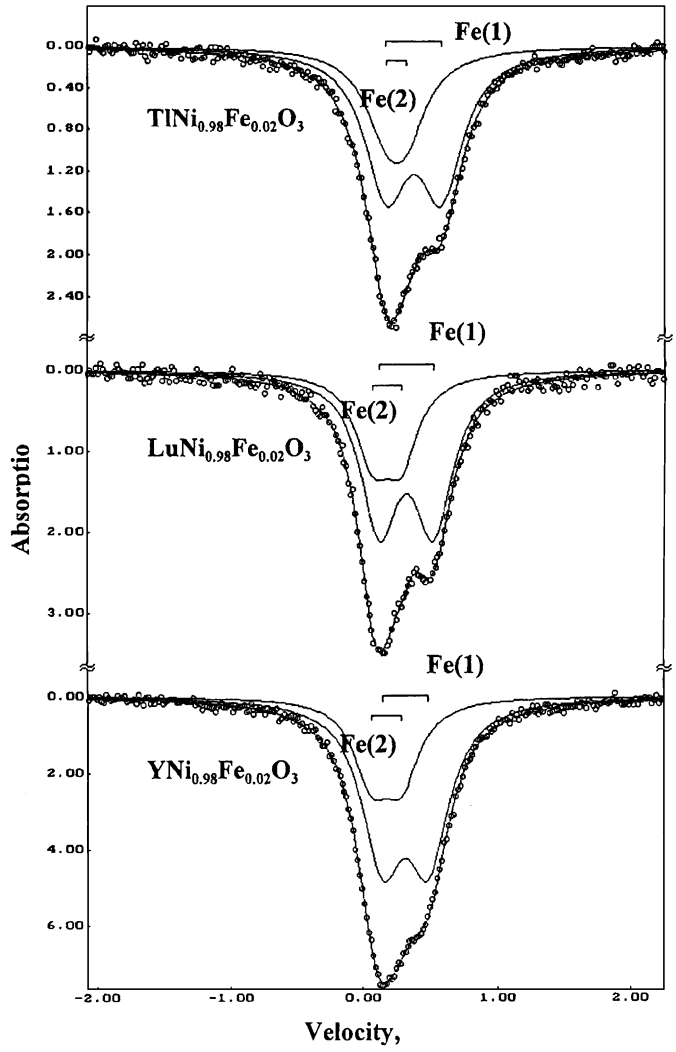

FIG. 4. ^{57}Fe Mössbauer spectra of $A\mathrm{Ni}_{0.98}{}^{57}\mathrm{Fe}_{0.02}\mathrm{O}_3$ (A = Tl, Lu, Y) at 300 K.

TABLE 2
Mössbauer Parameters for $A Ni_{0.98}{}^{57}Fe_{0.02}O_3$ (A = Y, Lu, Tl) at $T = 300$ K

Compounds	Fe-sites	δ (mm/s) (± 0.01)	Δ (mm/s) (± 0.01)	Γ (mm/s) (± 0.01)	S (%) ($\pm$ 2)
$YNi_{0.98}Fe_{0.02}O_3$	Fe(1)	0.32	0.34	0.30	67
	Fe(2)	0.18	0.23	0.31	33
$LuNi_{0.98}Fe_{0.02}O_3$	Fe(1)	0.31	0.38	0.31	66
	Fe(2)	0.15	0.21	0.30	34
$TlNi_{0.98}Fe_{0.02}O_3$	Fe(1)	0.36	0.40	0.30	67
	Fe(2)	0.23	0.18	0.31	33

TABLE 3
Valence, Degree of Charge Disproportionation of the Fe Probes, and Distortion of FeO_6 Octahedra in $A Ni_{0.98}{}^{57}Fe_{0.02}O_3$ Lattices (A = Y, Lu, Tl) at $T = 300$ K

Compounds	Fe-sites	N	$\langle n \rangle$	σ	$(\Delta_1/\Delta_2)_{exp}$	$(\Delta_1/\Delta_2)_{cal}$
$YNi_{0.98}Fe_{0.02}O_3$	Fe(1)	3.10	3.33	0.23	1.48	1.21
	Fe(2)	3.57		0.24		
$LuNi_{0.98}Fe_{0.02}O_3$	Fe(1)	3.13	3.38	0.25	1.80	1.45
	Fe(2)	3.67		0.29		
$TlNi_{0.98}Fe_{0.02}O_3$	Fe(1)	2.97	3.18	0.21	1.74	1.36
	Fe(2)	3.38		0.22		

However, this result is in a good agreement with the data of (4) where the authors showed that effective charges of Ni(1) and Ni(2) cations as well as $Ni(1)O_6$ and $Ni(2)O_6$ polyhedra sizes appear to be independent of the monoclinic distortion degree of the nickelates.

An analysis of experimental data for mixed-valence iron oxides containing heterovalent Fe^{3+}/Fe^{4+} cations with fast electron exchange reveals linear decrease of isomer shift with increase of average formal valence of iron (13). On the basis of average isomer shift values for high-spin Fe^{3+} (≈ 0.35 mm/s) and Fe^{4+} (≈ 0.05 mm/s) cations in octahedral $Fe^{n+}O_6$ polyhedra (13), the following empirical relation for intermediate high-spin Fe^{n+} states can be proposed:

$$\delta = 1.25 - 0.30n,$$

where δ is the room-temperature isomer shift with respect to α-Fe; n is the formal oxidation state ($3 \le n \le 4$) on a time scale $\tau > 10^{-8}$ s. Using the experimentally obtained $\delta_{1(2)}$ values (Table 2) the formal oxidation states for doped Fe^{n+} cations located in $Ni^{(3+\alpha)+}$ and $Ni^{(3-\alpha')+}$ positions in Lu, Y and Tl nickelates structure were calculated. The data thus obtained (Table 3) demonstrate a good correlation between the charge variation $\sigma = |\langle n \rangle - n|$ for Fe(1) and Fe(2) cations ($\langle n \rangle$: the average formal oxidation state of Fe(III) cations, which corresponds to the average isomer shift value: $(\delta_1 + \delta_2)/2$ (see Table 1) and the degree of charge disproportionation $\alpha(\alpha')$ for Ni(1) and Ni(2) ions (Table 4 and Fig. 5), the latter being determined using phenomenological Brown's bond-valence model (15). In addition, it should be noted that the effective charge variation $\sigma(\sigma')$ for Ni(1)/Ni(2) cations and $\alpha(\alpha')$ for Fe(1)/Fe(2) dopant cations calculated by independent methods do not reach the ideal values expected for a full disproportionation into Ni^{2+}/Ni^{4+} and Fe^{2+}/Fe^{4+}, respectively, but clearly indicate the differing chemical environments of the two sites.

The difference observed between quadrupole splittings for two types of iron $\Delta_1 > \Delta_2$ is in agreement with the neutron diffraction data (9), indicating that $Ni^{(3-\alpha')+}O_6$ polyhedra are more distorted than the $Ni^{(3+\alpha)+}O_6$ ones. The Δ_2/Δ_1 ratio obtained from Mössbauer spectra and that calculated for $Ni^{(3\pm\alpha)+}O_6$ polyhedra using point charge model support the above assumption (see Table 3). Some disagreement between theoretical and experimental data may reflect uncontrollable additional distortion of oxygen octahedra due to the size difference between Fe(III) and Ni(III). On the other hand, the point charge model is available in the case of isotropic electronic configuration Fe^{3+}: $3d^5$; when the iron real charge goes up to 3.57 or 3.67 as in the above nickelates, one has to take into account the electronic valence contribution of the *3d* shell to the EFG calculations (see below).

The temperature dependence of Mössbauer parameters (δ, Δ) for the two sub-spectra for Lu, Y, Tl nickelates are presented in Fig. 6. The δ_1 and δ_2 values for $LuNi_{0.98}Fe_{0.02}O_3$ increase monotonically with decreasing temperature due to the second-order Doppler effect. In the case of $YNi_{0.98}Fe_{0.02}O_3$, the parameters of both the sub-spectra are approximately the same within the experimental error. The above results suggest that the degree of charge variation for $Fe^{(\langle n \rangle - \sigma')+}(1)$ $Fe^{(\langle n \rangle + \sigma)+}(2)$ for the explored range of temperature in Lu, Y nickelates structure is temperature independent.

In the case of $TlNi_{0.98}Fe_{0.02}O_3$, the analysis of the spectrum at $T = 100$ K (Fig. 7) shows that the decrease of the temperature increases the difference between isomer shifts values for the two iron states: $\Delta\delta_{300\,K} = 0.13$ mm/s and $\Delta\delta_{100\,K} = 0.25$ mm/s, where $\Delta\delta = \delta_1 - \delta_2$. It should be

TABLE 4
Valence and Degree of Charge Disproportionation of the Ni Atoms in $ANiO_3$ Lattices (A = Y, Lu, Tl) at $T = 300$ K

Compounds	Ni-sites	n	$\langle n \rangle$	α	Ref.
$YNiO_3$	Ni(1)	2.62	2.89	0.27	(1, 9)
	Ni(2)	3.17		0.28	
$LuNiO_3$	Ni(1)	2.58	2.89	0.31	(1, 9)
	Ni(2)	3.24		0.35	
$TlNiO_3$	Ni(1)	2.54	2.89	0.35	—
	Ni(2)	3.07		0.18	

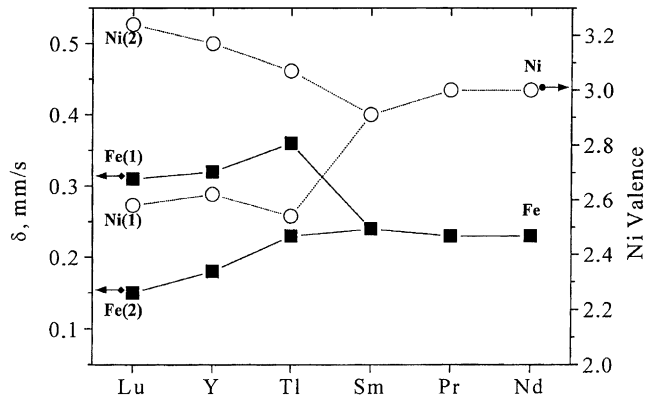

FIG. 5. Variation of the isomer shifts for ^{57}Fe(1) and ^{57}Fe(2) dopant atoms and valences for Ni(1) and Ni(2) as a function of rare earth (A) in ANi$_{0.98}{}^{57}$Fe$_{0.02}$O$_3$ (1, 9).

noted that only the isomer shift corresponding to Fe(1) cations (δ_1) changes substantially while the other one (δ_2) remains nearly the same (Fig. 8). The displacement of quadrupole doublets upon changing the temperature may be caused by two possible reasons. First, the second-order Doppler shift (δ_{soD}), which should lead to a shift of δ values into the positive velocities range for both iron states upon temperature decreasing. The second reason may be connected with the fact that degree of charge variation (σ) for $Fe^{(3+\sigma)+}$ and $Fe^{(3-\sigma')+}$ cations is temperature dependent. In contrast to $\delta_{\mathrm{soD}}(T)$, the increase of $\sigma(\sigma')$ has the opposite effect on δ value for the two types of iron cations: decreasing of δ_1 for Fe(1) and increasing of δ_2 for Fe(2) cations. In the case of $Fe^{(3+\sigma)+}$ cations partial compensation of second-order Doppler shift (δ_{soD}) and δ_σ caused by an increase of charge variation (σ) leads to a very small change of experimentally obtained δ_2 with decreasing temperature (Fig. 8). Using experimentally obtained $\delta_{1(2)}$ for both temperatures the values $\delta_{\mathrm{soD}} \approx 0.06$ mm/s and $\delta_\sigma \approx 0.04$ mm/s were estimated. The calculated δ_{soD} is to be related with $\delta_{\mathrm{soD}} = 0.08$ mm/s, determined from the average slope $d\delta/dT \approx -4.6 \times 10^{-4}$ mm/s K obtained for Pr, Nd, Sm nickelates. However, it should be noted that the above evaluations are only preliminary and for obtaining more accurate results the measuring of $\delta_{1(2)}(T)$ in a wide temperature range should be performed.

It is seen from Fig. 6 that in the case of Lu, Y, Tl nickelates the decrease of temperature leads to the increase of quadrupole splitting of both sub-spectra. Generally, the total EFG tensor principal component (eq_{exp}) at the nucleus of non-spherical ion consists of two contributions: eq^{lat} resulting from distortion of nearest lattice surrounding and eq^{val} arising from anisotropic electron populations in the anti-bonding molecular orbitals in FeO_6 polyhedra. The resulting quadrupole coupling constant $e^2q_{\mathrm{exp}}Q = 2\Delta$ for the iron cations being:

$$e^2q_{\mathrm{exp}}Q = eQ[eq^{\mathrm{lat}}(1-\gamma) + eq^{\mathrm{val}}(1-R)],$$

where γ and R are the corresponding Sternheimer anti-shielding and shielding factors, respectively.

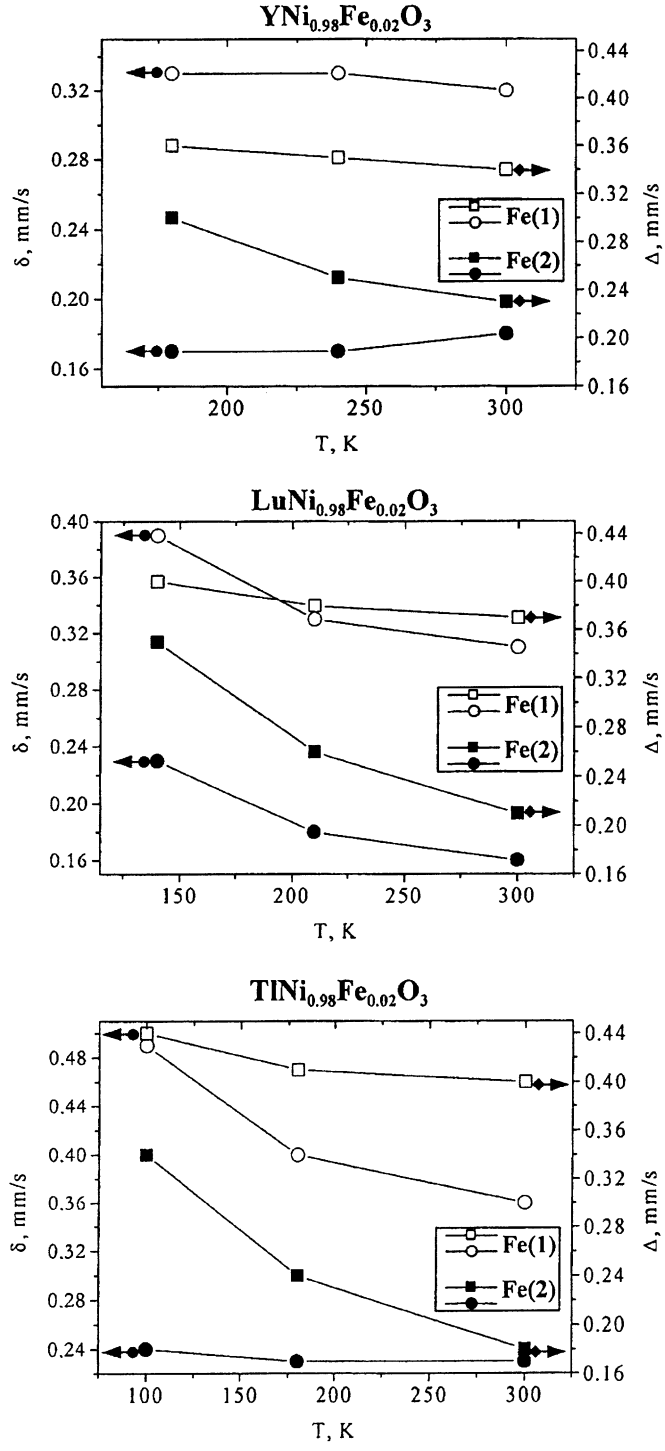

FIG. 6. Temperature dependence of Mössbauer parameters (δ, Δ) for Fe(1) and Fe(2) sub-spectra for Lu, Y and Tl nickelates.

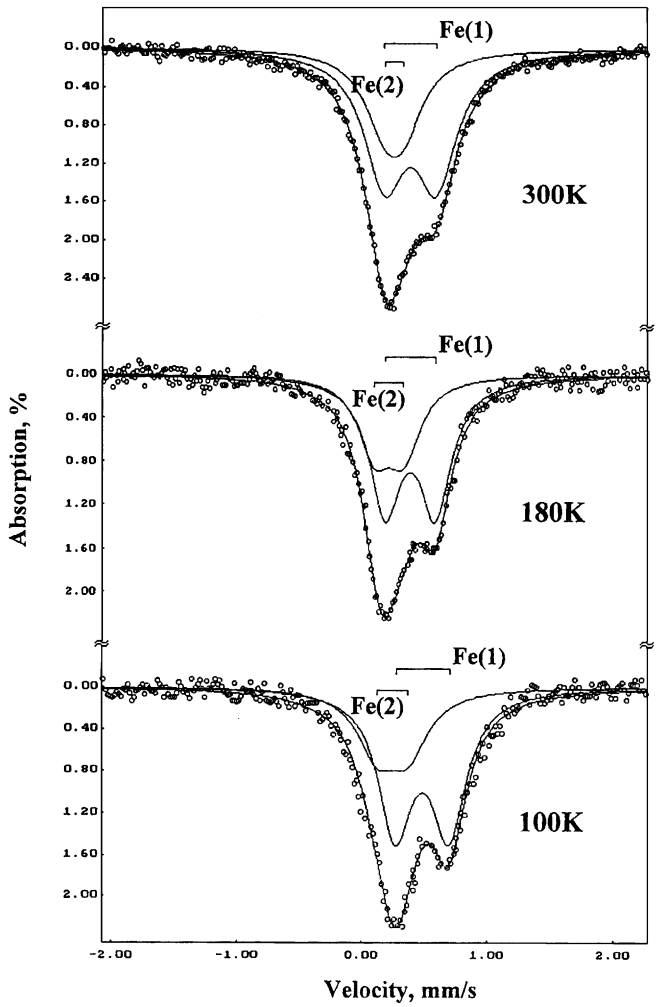

FIG. 7. ^{57}Fe Mössbauer spectra of $TlNi_{0.98}{}^{57}Fe_{0.02}O_3$ at 300, 180 and 100 K.

Unfortunately, there are no experimental data concerning the temperature dependence for distortion parameters of $Ni^{(3\pm\alpha)+}O_6$ polyhedra, which, in turn, contributes to eq^{lat}. However, in the case of the nickelates $ANiO_3$ (A = Lu, Y, Tl) no phase transitions were observed which were able to produce a substantial increase in eq^{lat} of the ^{57}Fe probe. Thus, the contribution of valent electrons of different types of iron cations is the main factor which provides the change of quadruple splitting for both the sub-spectra with decreasing temperature.

The high-spin trivalent iron cations in octahedral surrounding have the isotropic $t_{2g}^3e_g^2$ electron configuration, thus not contributing to eq^{val}. However, the expected stabilization of Fe(1) and Fe(2) cations in two $Ni^{(3\pm\alpha)+}O_6$ polyhedra will lead to the substantial deviation of ferric dopant electronic configuration from spherical symmetry. The structural distortion of both octahedrally coordinated FeO_6 sites in $ANi_{0.98}Fe_{0.02}O_3$ (A = Lu, Y and Tl) causes the unequal population of the d-levels for $Fe^{(3-\sigma')+}$(1) and $Fe^{(3+\sigma)+}$(2) cations. The population asymmetry would increase with decreasing temperature (according to Boltzmann distribution), and, consequently, the increase in eq^{val} value is to be expected. The temperature dependence of eq^{val} should be more substantial for Fe(2) cations, for which the charge variation (σ) leads to more changes in occupation of e_g^*-orbitals in comparison with the one for Fe(1) ions (Table 3).

In summary, Mössbauer spectroscopy investigations of $ANi_{0.98}{}^{57}Fe_{0.02}O_3$ (A = Lu, Y, Tl) at $T_N < T < T_t$ reveal the presence of ^{57}Fe dopant in two different sites, which could be assigned to $Fe^{(3+\sigma)+}$ and $Fe^{(3-\sigma')+}$. The analysis of temperature dependence of Lu, Y nickelates spectra shows that the charge variation (σ, σ') for dopant Fe(1) and Fe(2) cations does not depend on temperature. On the contrary, the changes of $TlNi_{0.98}Fe_{0.02}O_3$ spectra with decreasing temperature may be interpreted as dependence of $\sigma(\sigma')$ versus temperature. Such a result can be correlated to the weakening of the Ni(III)–O bond through the competition with the stronger covalent Tl^{III}–O bonds compared to the A^{III}–O ones (A = rare earth). The results obtained prove that using ^{57}Fe as probe atom, Mössbauer spectroscopy is

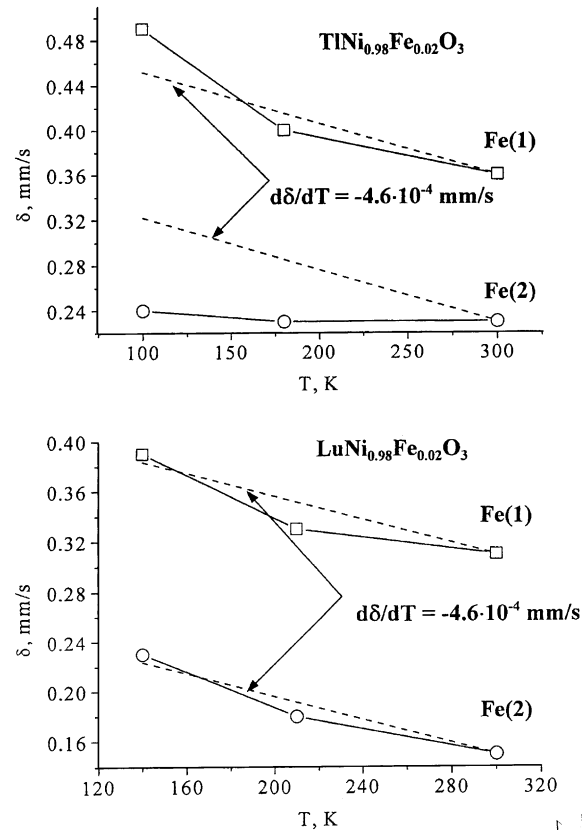

FIG. 8. Temperature dependence of the isomer shift (δ) for Fe(1) and Fe(2) sub-spectra for $ANi_{0.98}{}^{57}Fe_{0.02}O_3$ (A = Tl, Lu). The dashed lines are calculated from the average slope $d\delta/dT \approx -4.6 \times 10^{-4}$ mm/s K (see text).

particularly a useful tool for further investigations of temperature dependence of disproportionation as well as magnetic hyperfine interactions in magnetically ordered temperature range ($T < T_N$). High-temperature Mössbauer measurements ($T > T_t$) are currently under investigation to confirm our results.

REFERENCES

1. A. Wold, B. Post, and E. Banks, *J. Am. Chem. Soc.* **79,** 4911–4913 (1957).
2. G. Demazeau, A. Marbeuf, M. Pouchard, and P. Hagenmuller, *J. Solid State Chem.* **3,** 582–589 (1971).
3. S. J. Kim, G. Demazeau, J. A. Alonso, and J. H. Choy, *J. Mater. Chem.* **11,** 487–492 (2001).
4. M. L. Medarde, *J. Phys. Condens. Matter* **9,** 1679–1707 (1997).
5. J. B. Goodenough, A. Wold, R. J. Arnott, and N. Menyuk, *Phys. Rev.* **124,** 373–384 (1961).
6. J. Rodrigues-Carjaval, S. Rosenkranz, M. Medarde, P. Lacorre, M. T. Fernandez-Diaz, F. Fauth, and V. Trounov, *Phys. Rev. B* **57,** 456–464 (1998).
7. T. Takeda, R. Kanno, Y. Kanamotto, M. Takano, S. Kawasaki, T. Kamiyama, and F. Izumi, *Solid State Sci.* **2,** 673–687 (2000).
8. J. A. Alonso, M. J. Martinez-Lope, M. T. Casais, J. L. Garcia-Munoz, and M. T. Fernandez-Diaz, *Phys. Rev. B* **61,** 1756–1763 (2000).
9. J. A. Alonso, J. L. Garcia-Munoz, M. T. Fernandez-Diaz, M. A. G. Aranda, M. J. Martinez-Lope, and M. T. Casais, *Phys. Rev. Lett.* **82,** 3871–3874 (1999).
10. S. J. Kim, G. Demazeau, I. Presniakov, K. Pokholok, A. Sobolev, and N. Ovanesyan, *J. Am. Chem. Soc.* **123,** 8127–8128 (2001).
11. S. J. Kim, G. Demazeau, I. Presniakov, K. Pokholok, A. Sobolev, A. Baranov, D. Pankratov, and N. Ovanesyan, *Phys. Rev. B*, in press.
12. M. Eibschütz, S. Shtrikman, and D. Treves, *Phys. Rev.* **156,** 562 (1967).
13. F. Menil, *J. Phys. Chem. Solids* **46,** 763–789 (1985).
14. A. J. Boyle and H. E. Hall, *Rep. Prog. Phys.* **25,** 441 (1962).
15. I. D. Brown, *Z. Kristallogr.* **199,** 255–267 (1992).